Malaysian Journal of Analytical Sciences (MJAS)
Published by Malaysian Analytical Sciences Society

APPLICATION OF MAGNETIC BIO-POLYMER SPOROPOLLENIN AS LOW-COST ADSORBENT FOR REMEDIATION OF METHYLENE BLUE FROM AQUEOUS SOLUTION

(Aplikasi Magnetik Bio-Polimer Sporopollenin Sebagai Penjerap Kos-Rendah untuk Pemulihan Metilena Biru daripada Larutan Akueus)

Syed Fariq Fathullah Syed Yaacob[1,3*], Muhamad Zulfikry Shamsudin[1], Arniza Khairani Mohd Jamil[1], Faiz Bukhari Mohd Suah[3], and Sharifah Mohamad[1,2*]

[1]*Department of Chemistry, Faculty of Science, Universiti Malaya, 50603 Kuala Lumpur, Malaysia*
[2]*University Malaya Centre for Ionic Liquids (UMCiL), University of Malaya, 50603 Kuala Lumpur, Malaysia*
[3]*School of Chemical Sciences, Universiti Sains Malaysia, Pulau Pinang 11800, Malaysia*

[*]*Corresponding author: syedfariq@usm.my; sharifahm@um.edu.my*

Received: 28 September 2022; Accepted: 21 June 2023; Published: 22 August 2023

Abstract

Adsorption processes using low-cost sorbents such as bio-polymer adsorbents are an attractive option for removing methylene blue from wastewater. This study involved magnetic sporopollenin (MSp) synthesis and its application for removing methylene blue (MB) from an aqueous solution via adsorption process. The synthesized MSp was characterized by FT-IR and FESEM analyses. The effects of pH 2 - pH 8, sorbent dosage (10 mg - 50 mg), and contact time (0 - 60 min) were studied in batch mode and optimized. Adsorption isotherms models, Langmuir and Freundlich were used to simulate the equilibrium data. The Freundlich isotherm model is best fitted with the experimental data compared to the Langmuir model. A maximum absorption capacity (q_m) of 6.357 mg/g was obtained for MB. In addition, pseudo-first-order and pseudo-second-order were used to study the kinetics of MB adsorption onto MSp. The dye adsorption process obeyed the pseudo-second-order kinetic expression as proven by the high correlation coefficient (R^2 = 0.999). Overall, these findings confirmed the potential of MSp as an alternative and efficient sorbent for the removal of MB dye, offering promising prospects for wastewater treatment applications.

Keywords: magnetic nanoparticles, sporopollenin, methylene blue, isotherm, kinetics

Abstrak

Proses penjerapan menggunakan penjerap kos rendah seperti penjerap bio-polimer merupakan pilihan yang menarik untuk penyingkiran metilena biru daripada air sisa. Kajian ini melibatkan sintesis sporopollenin magnetik (MSp) dan aplikasinya untuk penyingkiran metilena biru (MB) daripada larutan akueus melalui proses penjerapan. MSp yang disintesis dicirikan oleh analisis FT-IR dan FESEM. Kesan pH 2 - pH 8, dos sorben (10 mg - 50 mg), dan masa dikaji (0 - 60 min) dalam mod kelompok dan dioptimumkan. Model isoterma penjerapan, Langmuir dan Freundlich digunakan untuk mensimulasikan data keseimbangan. Model isoterma Freundlich paling sesuai dengan data eksperimen berbanding dengan model Langmuir. Kapasiti penyerapan maksimum (q_m) sebanyak 6.357 mg/g diperolehi untuk MB. Di samping itu, pseudo-tertib pertama dan pseudo-tertib-kedua digunakan untuk mengkaji kinetik penjerapan MB ke MSp. Proses penjerapan pewarna mematuhi ekspresi kinetik pseudo-tertib-

kedua seperti yang dibuktikan oleh pekali korelasi tinggi (R^2 = 0.999). Secara keseluruhan, penemuan ini mengesahkan potensi MSp sebagai sorben alternatif dan cekap untuk penyingkiran pewarna MB, menawarkan prospek yang menjanjikan untuk aplikasi rawatan air sisa.

Kata kunci: magnetik nanopartikel, sporopollenin, metilena biru, isoterma, kinetik

Introduction

Recently, the abundance of pollutants in water has become a severe environmental issue. Amongst the industrial activities, dyeing industries are aggressively moving forward because of the extensive use of dyes in manufacturing industries, such as food, textile, paper, and plastic. Until now, more than 100,000 synthetic dyes have been produced, creating significant problems for the environment and human beings due to their toxicity and mutagenic effects [1]. The removal of synthetic dyes is an important concern as the incomplete degradation of dyes causes the production of carcinogenic and harmful amines [2]. Furthermore, the presence of color substances in the water may decrease light transmission and photosynthesis activity, leading to bacteria growth and hence inhibiting the growth of the plant and aquatic ecosystem in the water [3].

Methylene blue (MB) dye is a cationic dye commonly used in the industry's coloring processes. It also has broader applications, including usage as a temporary hair colorant, a colorant for cotton and wools, and a coating for paper stock. MB has been classified as a non-biodegradable dye and needs to be treated before being discharged into the environment [1]. MB can cause harmful side effects to humans, such as vomiting, shock, increased heart rate, and jaundice in newborn babies.

Many treatment techniques have been applied to different types of water and wastewater contaminated with dyes. These treatment techniques, include physical or chemical treatment processes. Treatment processes, include chemical coagulation [4], ozonation [5], oxidation [6], photodegradation [7], ion exchange [8], irradiation [9], nanofiltration [10], and adsorption [11]. Unfortunately, several of these techniques are costly, require various tools, and have limitations. Based on the literature [12], low-cost sorbent has been developed as an alternative for dye removal. Several low-cost adsorbents have been investigated for dye removal such as wood waste activated carbon [13], olive oil activated carbon [14], apricot stone activated carbon [15], weeds activated biochar [16], and ZnO-nano rods-activated carbon [17].

With the prevalence of adsorption as an essential technique for purifying dye-contaminated wastewater, the development of magnetic nanoparticles (MNPs) sorbent materials such as magnetite (Fe_3O_4) has gained notable recognition in water purification [18]. It is based on the advantages of having a simple manipulation process, high separation efficiency under an external magnetic field, and easy functional modifications for specificity and operation conditions [19]. Moreover, the high surface area-to-volume ratio properties possessed by MNPs ensure a better adsorption capacity and high recovery compared to other sorbents [20]. Nevertheless, adsorption also has a certain limitation that needs to be countered. For example, separation and recovery processes. After adsorption, separating the adsorbent from the solution can be challenging, especially when dealing with fine particles or colloidal materials. Thus, this process often requires additional filtration or centrifugation steps. Next, limitation is the environmental impact which some traditional adsorbents may have environmental implications due to their non-biodegradability or potential release of toxic substances during the adsorption process. Hence, these issues need to be countered properly.

Sporopollenin is a natural bio-polymer obtained from *Lycopodium clavatum*, which is highly resistant to chemical reactions, has a stable chemical structure and occurs naturally as a component of spore walls [21]. Furthermore, sporopollenin exhibits significant stability even after prolonged exposure to mineral acids and alkaline. Due to its efficiency and biocompatibility, sporopollenin is a well-known potential biomaterial used to remove various types of dye from the aqueous solutions. Sunset yellow [22], methyl orange [23], crystal violet [24] and Rhodamine B [25] have been successfully absorbed from an aqueous solution by

sporopollenin and its derivatives. Moreover, biopolymer sporopollenin is typically biodegradable, minimizing the environmental impact associated with the disposal of used adsorbents.

Sporopollenin loaded with magnetic functionality increases the total efficiency of the adsorption process and helps facilitate fast recovery. By incorporating magnetic nanoparticles or attaching magnetic moieties to the bio-polymer sporopollenin, it becomes responsive to external magnetic fields. This enables easy separation and recovery of the adsorbent from the solution by using a magnetic field, simplifying the overall process. Hence, a composite made from magnetic material is a suitable sorbent and thus a potential candidate for the removal of MB. A simple method for loading sporopollenin microcapsules with nanoparticles and insoluble salts is through a chemical reaction or a precipitation process that generates the encapsulated compounds inside the sporopollenin shell. This method produced magnetic sporopollenin loaded with magnetite nanoparticles and low solubility of organic salts [26].

Magnetic sporopollenin (MSp) was prepared as adsorbents in this study to remove MB dyes (Figure 1) from an aqueous solution. Two models, Langmuir and Freundlich, were used to describe the sorption process of MB adsorption onto the magnetic sporopollenin. Furthermore, the kinetics of MB adsorption onto the magnetic sporopollenin was investigated by using a pseudo-first-order and a pseudo-second-order models.

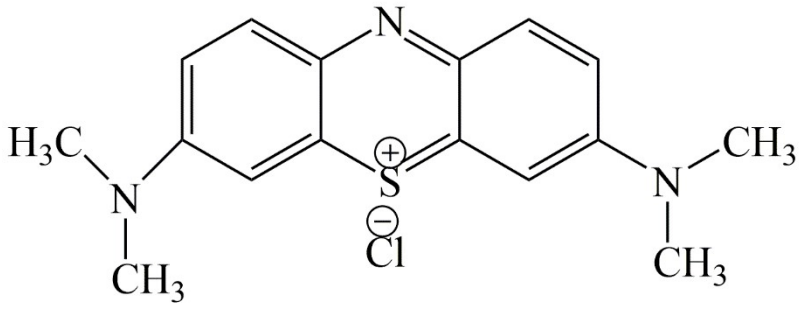

Figure 1. Structure of methylene blue (MB)

Materials and Methods

Materials

Analytical grade ammonia, ethanol, hydrochloric acid and sodium hydroxide pellet were purchased from Merck (Darmstadt, Germany) and used without further purification. Ferrous chloride tetrahydrate (CAS no. 13478-10-9) and ferric chloride hexahydrate (CAS no. 10025-77-1) were obtained from Sigma-Aldrich (Steinheim, Germany). All commercial grade solvents were stored over molecular sieves (4 Å, 8–12 mesh) from Aldrich (Steinheim, Germany). *Lycopodium clavatum* with a particle size of 25 µm was purchased from Aldrich (Steinheim, Germany). Methylene blue was obtained from Merck (Steinheim, Germany). The pH of the solution was adjusted by mixing an appropriate amount of HCl and/or NaOH (0.1 M). Deionized water that passed through a Milli-Q system (Lake End, UK) was used to prepare the solutions.

Instrumentation

Fourier transform infrared (FTIR) spectrometry (Spectrum 400 Perkin Elmer, Waltham, MA, USA) utilizing the ATR technique. Field emission scanning electron microscopy (FESEM) analysis was performed by using scanning electronic microscopy (HITACHI SU8220), OXFORD Instrument (Oxfordshire, UK). Ultraviolet-Visible (UV-Vis) spectrophotometer (Shimadzu, Tokyo, Japan) equipped with 1 cm quartz cells.

Preparation of magnetic sporopollenin (MSp)

MSp was prepared as follows: 13.32 g $FeCl_3.6H_2O$, 19.88 g $FeCl_2.4H_2O$, 5 mL of 5M HCl, 40 mL deionized water and 5 mL of ethanol were mixed in a 100 mL flask. The solution was stirred at room temperature until a complete dissolution of the salts. Then, 1.0 g of the

freshly prepared sporopollenin was redispersed in 30 mL of this solution and stirred for 2 h at room temperature. The sporopollenin suspension was filtered, and the filtrate was quickly washed with deionized water and immediately transferred to a 1.0 M ammonia solution. After 2 h stirring at room temperature, the MSp (with a core of magnetic nanoparticles) were collected by neodymium magnet, washed thoroughly with deionized water, and dried under vacuum. Figure 2 shows the preparation of MSp sorbent.

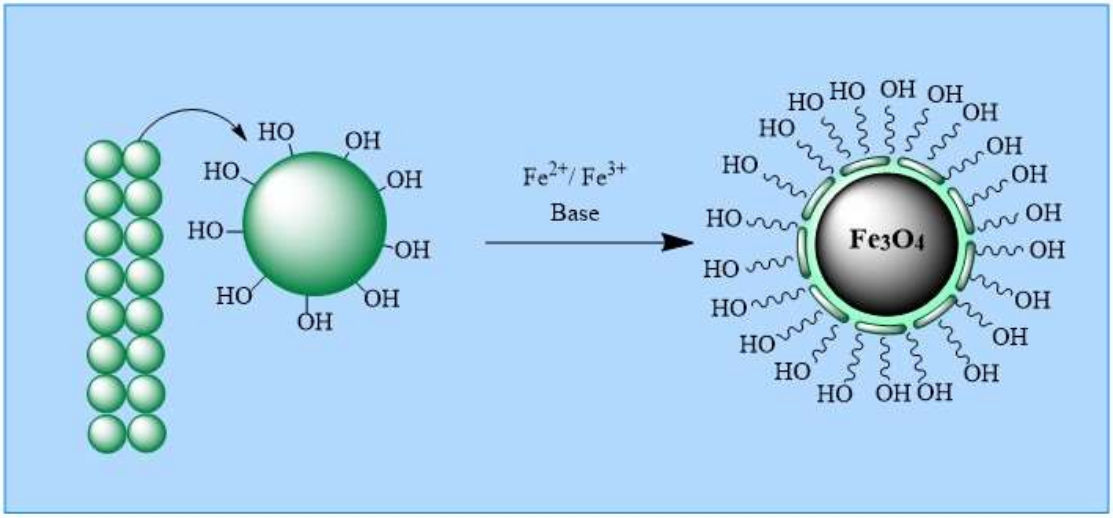

Figure 2. Synthesis of magnetic sporopollenin (MSp)

Sorption study

The batch sorption study was carried out to evaluate the MB removal efficiency of MSp sorbent. Different parameters, such as sorbent dosage (10 mg - 50 mg), pH (pH 2 - pH 8), and contact time (0 - 60 min) were optimized to achieve the optimum sorption results. The experiments were conducted in 25 mL Erlenmeyer flasks with glass caps containing the amount of the sorbent and concentration of sorbate solution, i.e., 5 ppm aqueous solution of MB. The Erlenmeyer flasks were stirred on a horizontal shaker operating at a constant speed (100 rpm) at room temperature for 10 min to obtain sorption equilibrium. Then, the sorbent was removed before measurement by using an external magnet. The MB concentration before the treatment and the residual concentration of MB in the aqueous phase after the treatment was analysed through UV-Vis spectrophotometer at 664 nm. The percentage removal and adsorption capacity of MB utilizing the synthesized MSp were calculated using Eq.1 and Eq.2, respectively. The percentage removal and q_e of MB were calculated through Eq. (1) as follows:

$$\frac{C_i - C_f}{C_i} \times 100\ \% \quad (1)$$

Where, C_i (mol L^{-1}) is initial concentration of MB before sorption, and C_f (mol L^{-1}) is final concentration of MB after adsorption.

$$q_e = \frac{V\,(C_0 - C_e)}{W} \quad (2)$$

Where, q_e is adsorption capacity (mg g^{-1}), V is aqueous volume (L), W is adsorption dosage (mg), and C_e (mol L^{-1}) and C_o (mol L^{-1}) are residual and initial concentrations of MB.

Results and Discussion

Characterization of adsorbent

The FTIR spectra provided information about the presence of functional groups. The FT-IR spectra for the synthesized MSp and sporopollenin were similar except for the characteristic peaks near 570 cm^{-1}, corresponding to (–Fe-O) bond stretching in Fe_3O_4. This characteristic peak showed that the sporopollenin was successfully magnetized with Fe_3O_4 [27]. The remaining peaks with their corresponding assignment were as follow: 3289 cm^{-1} (–OH), 1646 cm^{-1} (–C=O), 1546 cm^{-1} (–C=C), 1442 cm^{-1} (–C-C), 1260 cm^{-1} and 1113 cm^{-1} (–C-O) as shown in Figure 3.

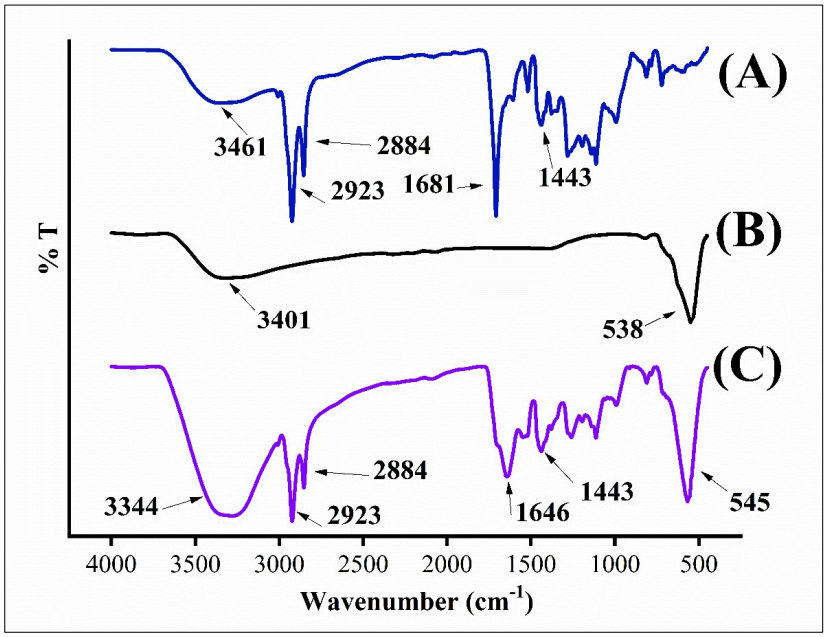

Figure 3. FTIR spectra of (a) raw Sp, (b) MNP, and (c) MSp

Field emission scanning electron microscopy (FESEM) is widely used to observe synthesized materials morphology and size distribution. FESEM images in Figure 4(a) show an open uniform pores structure and smooth surface morphology of sporopollenin. Meanwhile, Figure 4(b) shows a surface loaded with magnetic nanoparticles, which caused the change of porous structure to become limpid. This scenario confirmed that sporopollenin's surface has been successfully magnetized and was predominantly localized with magnetic nanoparticles [28].

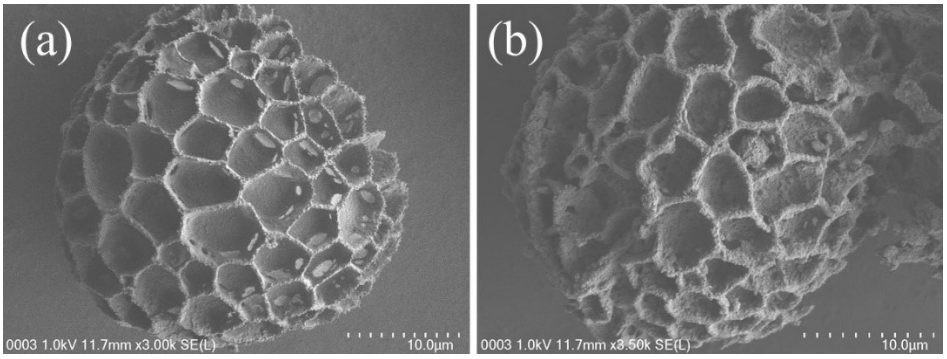

Figure 4. FESEM images of (a) sporopollenin and (b) MSp

Optimization of effective parameters on the removal of MB: Effect of sorbent dosage

Figure 4(a) shows the sorbent dosage's effect on MB adsorption. From the results, the percentage of MB removal increased rapidly from 61% to 90%, with increasing sorbent mass from 10 mg to 50 mg. The removal of MB was greater with the increase of sorbent dosage due to more available sites for adsorption. The amount of sorbent for further adsorption experiments was selected as 30 mg because beyond this point; there was no signification increase in adsorption of the MB. Therefore, all experiments were carried out with a fixed amount of 30 mg sorbent.

Effect of solution pH

This study investigated the effect of solution pH on the removal of MB (Figure 5b) at different pH ranges. The removal of MB increased with the pH of the solution from pH 2 to pH 8. Above pH 8, the removal of MB reached an equilibrium. This was due to the cation exchange between the sorbent and dye solution. The reported pH_{zpc} for MNP was pH 6.5 [29]. Beyond the pH_{zpc} point, the sorbent surface was in its protonated form, resulting in electrostatic repulsion between the positively charged MB and the sorbent surface. The higher amount of hydrogen ions in the solution prevented the negative charge formation on the MSp surface; thus, reducing the dye uptake. Above the pH_{zpc} point, the sorbent surface deprotonated the hydroxyl groups on the surface of MSp and provided more negative sites for electrostatic attraction between the cationic form of the dye molecules and the sorbent surface. Percentage removal was higher at this point; thus, the optimum pH for the maximum adsorption capacity of MB was determined to be pH 8.

Effect of contact time

Figure 5(c) shows that the amount of MB adsorbed (mg/g) increased with the contact time as predicted. During the first 5 min of the adsorption process, the percentage removal rapidly increased. As the contact time increased to 10 min, the adsorption of MB dye reached a maximum level and achieved an equilibrium. By further increment from 10 min to 60 min, the percentage of removal showed no significant changes that could be due to saturated binding sites on surface of MSp. Thus, 10 min was sufficient for removing MB and selected as the optimum contact time for further analysis.

Sorption isotherm

Adsorption isotherms described how analytes interact with sorbent materials in optimizing adsorbents. Therefore, the relationship between the removal ability of the material and the concentration of the contaminant solution can be illustrated by adsorption isotherms. It is crucial to establish the most appropriate correlation for the equilibrium curve to optimize the design of an adsorption system to remove dye from the solutions [30]. The investigation of the adsorption process was employed by Langmuir and Freundlich isotherm models. Furthermore, linearized forms of their equations have been used to describe the isotherm curves. The relative parameters of each equation were obtained by using the linear regressive analysis. In this study, the adsorption isotherm of MB by MSp was measured by shaking it for 10 min at different initial concentrations at pH 8 at room temperature.

The Langmuir isotherm suggested that sorption occurred on a homogeneous surface to obtain maximum adsorption capacity. No further adsorption process will occur if a solute occupies the site [31-32]. Langmuir isotherm models assumed the sorbate's monolayer coverage on a sorbent surface at a constant temperature. The linear fit of Langmuir for the adsorption of MB onto MSp is shown in Figure 6(a). The following equation represents the Langmuir isotherm:

$$\frac{C_e}{q_e} = \frac{C_e}{q_m} + \frac{1}{q_m b} \quad (3)$$

Where q_e is amount of solute sorbed on the surface of the sorbent, C_e is equilibrium ion concentration in the solution, q_m is maximum surface density at monolayer coverage, and b is Langmuir adsorption constant. The plot of $\frac{C_e}{q_e}$ vs. C_e for the sorption gives a straight line of slope $\frac{1}{q_o}$ (Figure 6a).

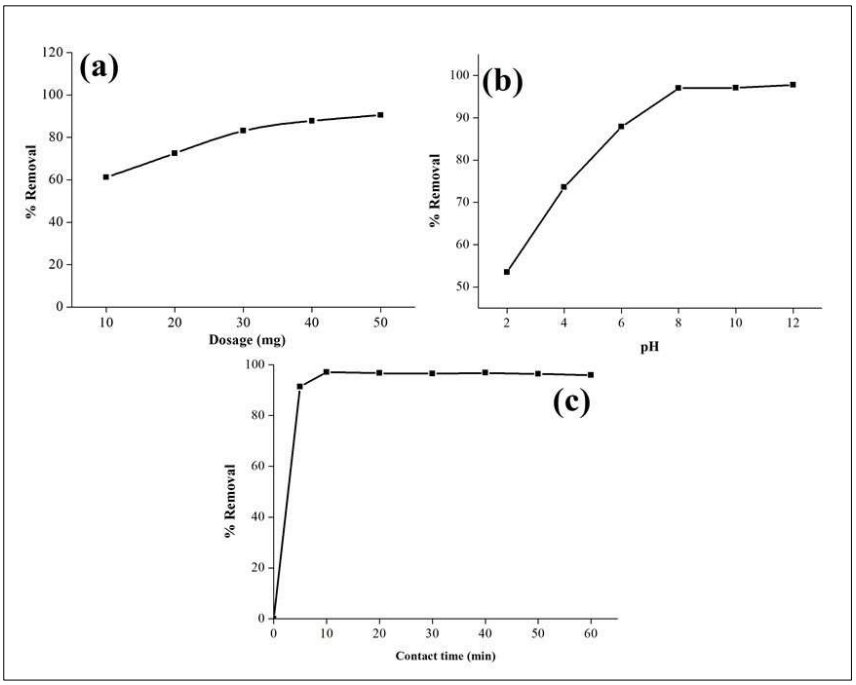

Figure 5. The effect of (a) dosage, (b) pH, and (c) contact time on the sorption of MB

The value of q_m, b and R^2 are presented in Table 1. The results indicated that the linear form of the Langmuir model showed a minimal deviation from the fitted equation as indicated by the R^2 value of 0.9637. This result suggested that the Langmuir model could not describe the relationship between the adsorbed amount of MB and its equilibrium concentration in the solution. Hence, the adsorption data would not follow the Langmuir model as compared to the Freundlich model.

Freundlich isotherm model suggested the sorbent surface heterogeneity with different energy of active sites and reversible adsorption which is restricted to multilayer formation. The Freundlich isotherm equation is shown as below:

$$\log q_e = \log K_F + \frac{1}{n}\log C_e \quad (4)$$

Where K_F and n are Freundlich constants related to the adsorption capacity and adsorption intensity, respectively. q_e is equilibrium solute concentration on sorbent, and C_e is equilibrium concentration of the solute.

The linear plot of $logq_e$ versus $logC_e$ for the Freundlich isotherm is shown in Figure 6(b). The constants of K_F and $1/n$ can be evaluated from the intercept and slope of the linear plot of experimental data are shown in Table 1. A larger value of K_F indicates the greater adsorption capacity while n values indicate the favourability of the adsorption process. If n is above unity, then the adsorption process is favourable.

The Freundlich isotherm plot was found to be linear over the studied concentration range, and the correlation coefficient (R^2 = 0.9988) obtained was higher than the Langmuir isotherm model. In addition, the Freundlich constant, K_F was 82.38 L/mg. In the present study, the value of n (indicative of favorability) is 1.476, which is above unity, indicating the favourability of the adsorption process. This showed that the interaction force between the MB dye and MSp sorbent was strong. Therefore, the Freundlich model is a good model to describe the adsorption data. The applicability of the

Freundlich adsorption model proposed the multilayer coverage of MB dye on the surface of MSp. Hence, the Freundlich model's experimental data indicated that the MSp surface's nature is heterogeneous with different adsorption sites.

Similarly, Boukhemkhem and Rida [33] reported a good adsorption potential (n = 4.17) for MB uptake modified Tamazert kaolin. The Freundlich model best fits to describe the adsorption of MB onto Tamazert kaolin relative to the Langmuir isotherm models implying multilayer adsorption onto a heterogeneous surface. In contrast, Mosleh and co-workers [34] reported magnetic sporopollenin supported polyaniline (MSP-PANI) for removal of lead ion (Pb^{2+}) was suitable for Langmuir isotherm with the maximum adsorption capacity of 163 mg/g and followed the monolayer pattern. Similarly, for magnetic sporopollenin supported magnesium nanocomposite (MSP@MgO) for removal of tetracycline (TCP) reported by Algethami and co-workers [35]. The adsorption models were investigated, and the process was fitted with the Langmuir model with adsorption capacities of 110 mg/g. Overall, the isotherm mechanism depended on the nature of the interactions between the adsorbent and the adsorbate.

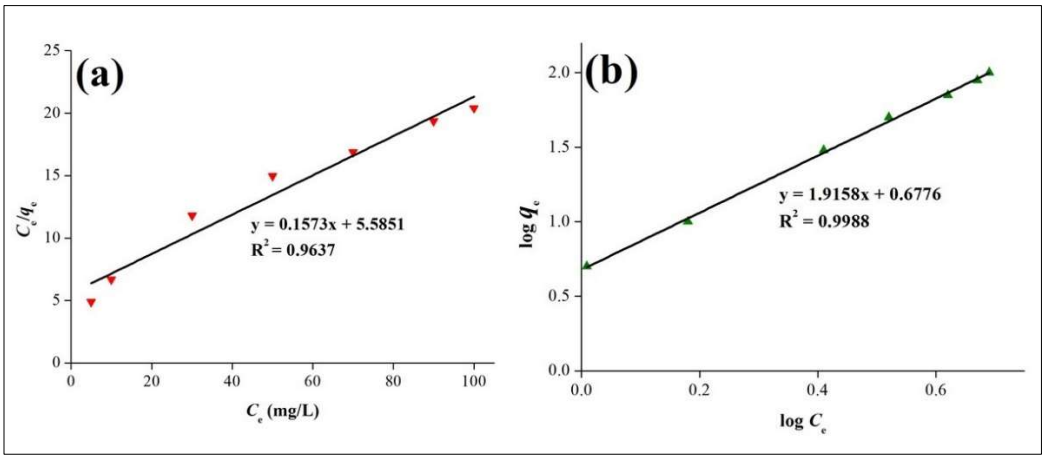

Figure 6. (a) Langmuir isotherms; (b) Freundlich isotherms for removal of MB by MSp

Table 1. Isotherm constants and regression data for adsorption of MB onto MSp at room temperature

Langmuir Constant			Freundlich Constant		
q_m (mg/g)	b (L/mg)	R^2	K_F (L/mg)	n	R^2
6.357	0.027	0.9637	82.38	1.476	0.9988

Sorption kinetics

Adsorption kinetics can describe a relationship between the amount of MB dye adsorbed to MSp in the aqueous solution. The analysis of the kinetic data is essential to generate an equation that accurately represents the results and could be used for design purposes [36]. The adsorption of MB dye onto MSp was further studied in terms of the kinetic model via pseudo-first-order and pseudo-second-order equations. The boundary layer resistance will be affected by the rate of adsorption with an increase in the contact time, which will increase the mobility of the adsorbate during adsorption. Since the uptake of adsorbates at the active sites of MSp is a rapid process, the adsorption rate is governed mainly by either the liquid phase mass transfer or the rate of intraparticle mass transfer.

Pseudo-first-order model

The pseudo-first-order model rate is based on the sorption capacity of the sorbent. The first-order model is

extensively applied for the adsorption of any solute from solution by the standard exchange procedure, which is fast and is mainly controlled by diffusion [37]. The plots of log ($q_e - q_t$) versus *t* are shown in Figure 7. The pseudo-first-order equation is expressed as:

$$log\ (q_e - q_t) = log\ q_e - K_1 t \quad (5)$$

Where, q_e and q_t are amounts of MB (mg g^{-1}) absorbed at equilibrium and at the time, *t,* respectively and K_1 is first order rate constant (min^{-1}). The values of q_e and K_1 are obtained from the linearity of pseudo-first-order rate by plotting $log\ (q_e - q_t)$ versus time, *t*.

The rate constant, K_1 and q_e are tabulated in Table 2. From Table 2, the value of R^2 = 0.7465 was low. Also, the calculated equilibrium adsorption capacities ($q_{e\ cal}$) by MSp was 0.276 mg/g, which is not consistent with the experimental data (q_e = 4.855 mg/g); hence this value is not in good agreement. This showed that the adsorption of MB onto MSp is not based on first-order kinetics.

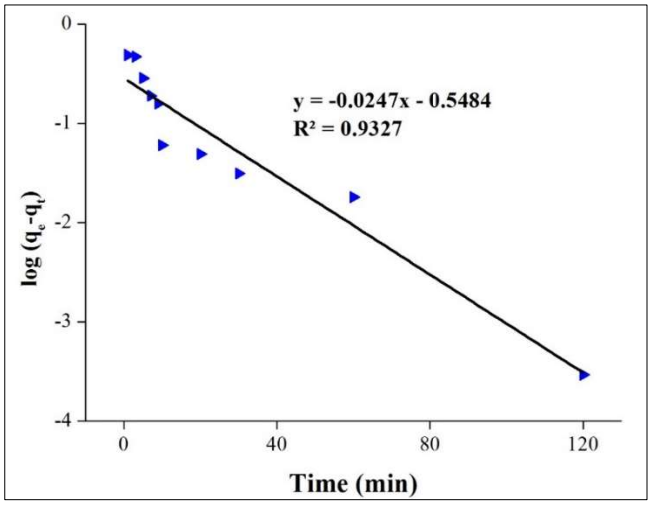

Figure 7. Pseudo-first order kinetic of MB.

Pseudo-second-order model

On the other hand, the pseudo-second-order model proposes that chemisorption is the rate-limiting step and that adsorption occurs on localized sites where no interactions between adsorbates arise [36]. Figure 8 shows the linear plots for the initial concentration studied.

The pseudo-second-order kinetic model applied for analyzing chemisorption kinetics from liquid solutions can be represented by Eq. (6) as follows.

$$\frac{t}{q_t} = \frac{1}{K_2 q_e^2} + \frac{t}{q_e} \quad (6)$$

Where K_2 is rate constant of pseudo-second-order adsorption (g/mg min). The value of K_2 and q_e can be described from the slope and the intercept of the graph $\frac{t}{q_t}$ versus t, respectively.

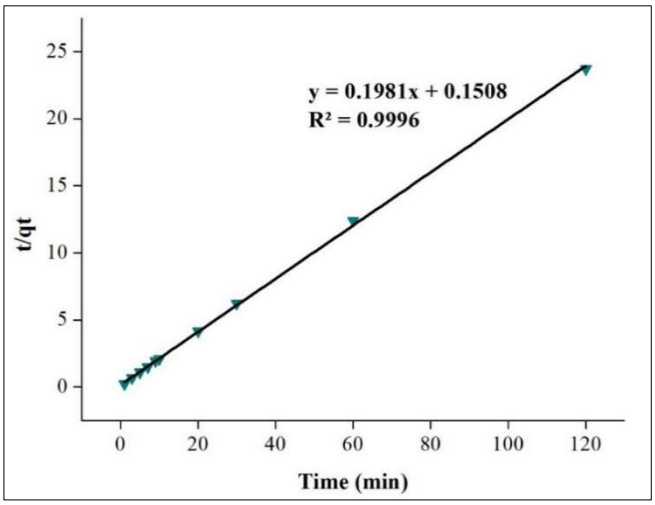

Figure 8. Pseudo-second order kinetic of MB

From Table. 2, the correlation coefficient (R^2) for the pseudo-second-order model is better (0.9996) than the pseudo-first-order model. The calculated equilibrium adsorption capacities ($q_{e\,cal}$) by MSp was found to be 4.684 mg/g, which is consistent with the experimental data ($q_{e\,exp}$ = 4.855 mg/g). A comparison between the calculated ($q_{e\,cal}$) and experimental ($q_{e\,exp}$) adsorption capacities revealed the pseudo-second-order model high applicability to describe the sorption process. Hence, the adsorption of MB onto MSp indicated that the adsorption kinetic is better represented by the pseudo-second-order model. Because of these results, it can be said that the pseudo-second-order kinetic model provided a good correlation for the adsorption of MB onto MSp in contrast to the pseudo-first-order model. This trend showed that the electron sharing between adsorbate and adsorbent is suited to uptake MB from aqueous media with high efficiency [38]. Numerous authors have reported similar pseudo-second-order kinetics, for adsorption of MB on different adsorbents, such as polyvinyl alcohol/carboxymethyl cellulose isolated from pineapple peel (PVA/CMC/GO/bentonite) [39], carboxymethyl cellulose-acrylamide-graphene oxide (CMC/AAm-GO) [40], and chitosan-g-poly(acrylic acid) modified cellulose nanowhiskers (Chitosan-g-PAA/CNW) [41].

Table 2. Kinetic parameters for adsorption of MB onto MSp

C_0	$q_{e\,exp}$ (mg/g)	Pseudo-First-Order Model			Pseudo-Second-Order Model		
		q_e (mg/g)	K_1 (1/min)	R^2	q_e (mg/g)	K_2	R^2
30	4.855	0.276	0.055	0.7465	4.684	0.855	0.9996

Comparison of sorption capacities of MSp with other adsorbents for MB removal

A comparison between MSp and other reported adsorbents in the literature is listed in Table 3. The performances were evaluated regarding the adsorption capacities. The data showed that the sorption capacity of MSp is relatively high as compared to other common sorbents except for several adsorbents such as spent rice biomass.

Table 3. The sorption capacities of the proposed MSp compared to other common adsorbents for the removal of MB

Adsorbent	Type of Analyte	Sorption Capacities (mg/g)	Ref
Glass wool	MB	2.20	[42]
Cashew nutshell	MB	5.31	[43]
Pyrolyzed petrified sediment	MB	2.39	[44]
Spent rice biomass	MB	8.30	[45]
Coir pith carbon	MB	5.87	[46]
Mansonia wood sawdust	MB	15.32	[47]
Padina sanctae-crucis	Methyl violet	10.02	[48]
Calcined lotus leaf	Methyl violet	26.32	[49]
Walnut shells	MB & methyl violet	6.5	[50]
Magnetic sporopollenin (MSp)	MB	6.4	This study

Conclusion

This study offered a unique method for removing methylene blue (MB) from aqueous solutions by implementing the economical adsorbent magnetic bio-polymer sporopollenin (MSp). The successful synthesis of MSp is confirmed by characterization by using FESEM analysis and FTIR spectroscopy. The optimum adsorption capacity of MB was achieved, and investigation of adsorption mechanisms sorption isotherms and isotherm kinetics revealed the Freundlich model and pseudo-second-order providing the best fit with the multilayer sorption on a heterogeneous surface. Some future prospects can be considered, including incorporating sporopollenin into polymer-based matrices, such as hydrogels or composite materials, to create hybrid adsorbents. The porous nature and flexibility of polymer matrices can enhance the adsorption capacity and stability of sporopollenin, making it suitable for various applications. Additional isotherm models, such as the Temkin model, Hasley model and Dubinin-Radushkevich isotherms model can be done to provide further insights into the adsorption behavior of methylene blue. These models can help characterize the energetic heterogeneity of the adsorbent surface, assess the feasibility of adsorption processes, and improve the understanding of the adsorption mechanisms. Lastly, in terms of regeneration and reusability to investigate the regeneration potential of MSp after MB adsorption. This is to ensure the restoration of the adsorption capacity of MSp, allowing for its repeated use and reducing overall operational costs.

Acknowledgement

Authors would like to acknowledge the valuable support from the University of Malaya Research Grants (Project No RP020A-16SUS), (Project No RG381-17AFR), (Project No. PG046-2015A), and the Ministry of Higher Education for scholarship (MyBrain15) provided.

References

1. Mazzeo, L., Marzi, D., Bavasso, I., Bracciale, M. P., Piemonte, V., and Di Palma, L. (2022). Characterization of waste roots from the as hyperaccumulator *Pteris vittata* as low-cost adsorbent for methylene blue removal. *Chemical Engineering Research and Design,* 186: 13-21.
2. Lade, H., Kadam, A., Paul, D., and Govindwar, S. (2015). Biodegradation and detoxification of textile azo dyes by bacterial consortium under sequential microaerophilic/aerobic processes. *EXCLI Journal,* 14: 158-174.
3. Durrani, W. Z., Nasrullah, A., Khan, A. S., Fagieh, T. M., Bakhsh, E. M., Akhtar, K., Khan, S. B., Din, I. U., Khan, M. A., and Bokhari, A. (2022). Adsorption efficiency of date palm based activated carbon-alginate membrane for methylene blue. *Chemosphere,* 302: 134793.
4. Sadri Moghaddam, S., Alavi Moghaddam, M. R., and Arami, M. (2010). Coagulation/flocculation process for dye removal using sludge from water treatment plant: Optimization through response surface methodology. *Journal of Hazardous Materials,* 175(1): 651-657.

5. Sripiboon, S., and Suwannahong, K. (2018). Color removal by ozonation process in biological wastewater treatment from the breweries. *IOP Conference Series: Earth and Environmental Science,* 167: 012010.
6. Khalaf, R. M., Kariem, N. O., and Khudhair, A. A. M. (2018). Removal of textile dye from aqueous media using an advanced oxidation process with UV/H_2O_2. *IOP Conference Series: Materials Science and Engineering,* 433: 012039.
7. Soltani, N., Saion, E., Hussein, M.Z., Erfani, M., Abedini, A., Bahmanrokh, G., Navasery, M., and Vaziri, P. (2012). Visible light-induced degradation of methylene blue in the presence of photocatalytic ZnS and CdS nanoparticles. *International Journal of Molecular Sciences,* 13(10): 12242-12258.
8. Huang, R., Zhang, Q., Yao, H., Lu, X., Zhou, Q., and Yan, D. (2021). Ion-exchange resins for efficient removal of colorants in bis(hydroxyethyl) terephthalate. *ACS Omega,* 6(18): 12351-12360.
9. Son, G., and Lee, H. (2016). Methylene blue removal by submerged plasma irradiation system in the presence of persulfate. *Environmental Science and Pollution Research,* 23(15): 15651-15656.
10. Cheng, S., Oatley, D. L., Williams, P. M., and Wright, C. J. (2012). Characterization and application of a novel positively charged nanofiltration membrane for the treatment of textile industry wastewaters. *Water Research,* 46(1): 33-42.
11. Tharaneedhar, V., Senthil Kumar, P., Saravanan, A., Ravikumar, C., and Jaikumar, V. (2017). Prediction and interpretation of adsorption parameters for the sequestration of methylene blue dye from aqueous solution using microwave assisted corncob activated carbon. *Sustainable Materials and Technologies,* 11: 1-11.
12. Ighalo, J. O., Omoarukhe, F. O., Ojukwu, V. E., Iwuozor, K. O., and Igwegbe, C. A. (2022). Cost of adsorbent preparation and usage in wastewater treatment: A review. *Cleaner Chemical Engineering,* 3: 100042.
13. Kaith, B. S., Dhiman, J., and Kaur Bhatia, J. (2015). Preparation and application of grafted Holarrhena antidycentrica fiber as cation exchanger for adsorption of dye from aqueous solution. *Journal of Environmental Chemical Engineering,* 3(2): 1038-1046.
14. Hazzaa, R., and Hussein, M. (2015). Adsorption of cationic dye from aqueous solution onto activated carbon prepared from olive stones. *Environmental Technology & Innovation,* 4: 36-51.
15. Djilani, C., Zaghdoudi, R., Djazi, F., Bouchekima, B., Lallam, A., Modarressi, A., and Rogalski, M. (2015). Adsorption of dyes on activated carbon prepared from apricot stones and commercial activated carbon. *Journal of the Taiwan Institute of Chemical Engineers,* 53: 112-121.
16. Güzel, F., Sayğılı, H., Akkaya Sayğılı, G., Koyuncu, F., and Yılmaz, C. (2017). Optimal oxidation with nitric acid of biochar derived from pyrolysis of weeds and its application in removal of hazardous dye methylene blue from aqueous solution. *Journal of Cleaner Production,* 144: 260-265.
17. Dil, E. A., Ghaedi, M., Ghaedi, A. M., Asfaram, A., Goudarzi, A., Hajati, S., Soylak, M., Agarwal, S., and Gupta, V. K. (2016). Modeling of quaternary dyes adsorption onto ZnO–NR–AC artificial neural network: Analysis by derivative spectrophotometry. *Journal of Industrial and Engineering Chemistry,* 34: 186-197.
18. Nodehi, R., Shayesteh, H., and Rahbar-Kelishami, A. (2022). Fe_3O_4@NiO core–shell magnetic nanoparticle for highly efficient removal of Alizarin red S anionic dye. *International Journal of Environmental Science and Technology,* 19(4): 2899-2912.
19. Yaacob, S. F. F. S., Jamil, A. K. M., Kamboh, M. A., Ibrahim, W. A. W., and Mohamad, S. (2018). Fabrication of calixarene-grafted bio-polymeric magnetic composites for magnetic solid phase extraction of non-steroidal anti-inflammatory drugs in water samples. *PeerJ, 6*: e5108.
20. Yaacob, S. F. F. S., Abd Razak, N. S., Aun, T. T., Rozi, S. K. M., Jamil, A. K. M., and Mohamad, S. (2018). Synthesis and characterizations of magnetic bio-material sporopollenin for the removal of oil from aqueous environment. *Industrial Crops and Products,* 124: 442-448.
21. Yaacob, S. F. F. S., Jamil, R. Z. R., and Suah, F. B. M. (2022). Sporopollenin based materials as a

versatile choice for the detoxification of environmental pollutants—A review. *International Journal of Biological Macromolecules*, 207: 900-1004.

22. Bişgin, A. T., Nalvuran, Z., and Gezici, O. (2021). Simultaneous preconcentration and spectrophotometric determination of two colorants (E110 and E133) in some foodstuffs using a new mussel-inspired adsorbent. *Journal of AOAC International,* 104(1): 137-147.
23. Ayar, A., Gezici, O., and Küçükosmanoğlu, M. (2007). Adsorptive removal of methylene blue and methyl orange from aqueous media by carboxylated diaminoethane sporopollenin: On the usability of an aminocarboxilic acid functionality-bearing solid-stationary phase in column techniques. *Journal of Hazardous Materials,* 146(1): 186-193.
24. Gezici, O., Küçükosmanoğlu, M., and Ayar, A. (2006). The adsorption behavior of crystal violet in functionalized sporopollenin-mediated column arrangements. *Journal of Colloid and Interface Science,* 304(2): 307-316.
25. Ecer, Ü., Şahan, T., Zengin, A., and Gubbuk, İ. H. (2022). Decolorization of Rhodamine B by silver nanoparticle–loaded magnetic sporopollenin: characterization and process optimization. *Environmental Science and Pollution Research*, 29(52): 79375-79387.
26. Ahmad, N. F., Kamboh, M. A., Nodeh, H. R., Halim, S. N. B. A., and Mohamad, S. (2017). Synthesis of piperazine functionalized magnetic sporopollenin: a new organic-inorganic hybrid material for the removal of lead(II) and arsenic(III) from aqueous solution. *Environmental Science and Pollution Research,* 24(27): 21846-21858.
27. Kamboh, M. A., and Yilmaz, M. (2013). Synthesis of N-methylglucamine functionalized calix [4] arene based magnetic sporopollenin for the removal of boron from aqueous environment. *Desalination,* 310: 67-74.
28. Yilmaz, E. (2012). Enantioselective enzymatic hydrolysis of racemic drugs by encapsulation in sol–gel magnetic sporopollenin. *Bioprocess and Biosystems Engineering,* 35(4): 493-502.
29. Khoeini Sharifabadi, M., Saber-Tehrani, M., Waqif Husain, S., Mehdinia, A., and Aberoomand-Azar, P. (2014). Determination of residual nonsteroidal anti-inflammatory drugs in aqueous sample using magnetic nanoparticles modified with cetyltrimethylammonium bromide by high performance liquid chromatography. *The Scientific World Journal,* 2014: 127835.
30. Dąbrowski, A. (2001). Adsorption—from theory to practice. *Advances in Colloid and Interface Science,* 93(1-3): 135-224.
31. Mehmood, T., Khan, A. U., Raj Dandamudi, K. P., Deng, S., Helal, M. H., Ali, H. M., and Ahmad, Z. (2022). Oil tea shell synthesized biochar adsorptive utilization for the nitrate removal from aqueous media. *Chemosphere,* 307: 136045.
32. Gao, Z., Wang, J., Muhammad, Y., Hu, P., Hu, Y., Chu, Z., Zhao, Z., and Zhao, Z. (2022). Hydrophobic shell structured NH2-MIL(Ti)-125@mesoporous carbon composite via confined growth strategy for ultra-high selective adsorption of toluene under highly humid environment. *Chemical Engineering Journal,* 432: 134340.
33. Boukhemkhem, A., and Rida, K. (2017). Improvement adsorption capacity of methylene blue onto modified Tamazert kaolin. *Adsorption Science & Technology*, 35(9-10): 753-773.
34. Mosleh, N., Najmi, M., Parandi, E., Nodeh, H. R., Vasseghian, Y., and Rezania, S. (2022). Magnetic sporopollenin supported polyaniline developed for removal of lead ions from wastewater: Kinetic, isotherm and thermodynamic studies. *Chemosphere*, 300: 134461.
35. Algethami, J. S., Yadav, K. K., Gacem, A., Ali, I. H., Rezania, S., Alhar, M. S. O., Mezni, A., Jeon, B. H., and Chaiprapat, S. (2023). Magnetic sporopollenin supported magnesium nanoparticles for removal of tetracycline as an emerging contaminant from water. *Environmental Science and Pollution Research*, 2023: 1-12.
36. Ho, Y. S., and McKay, G. (1999). Pseudo-second order model for sorption processes. *Process Biochemistry,* 34(5): 451-465.
37. Reçber, Z. B., Burhan, H., Bayat, R., Nas, M. S., Calimli, M. H., Demirbas, Ö., Şen, F., and Hassan, K.-M. (2022). Fabrication of activated carbon supported modified with bimetallic-platin ruthenium nano sorbent for removal of azo dye

from aqueous media using enhanced ultrasonic wave. *Environmental Pollution,* 302: 119033.

38. Lyu, F., Niu, S., Wang, L., Liu, R., Sun, W., and He, D. (2021). Efficient removal of Pb(II) ions from aqueous solution by modified red mud. *Journal of Hazardous Materials*, 406: 124678.
39. Dai, H., Huang, Y., and Huang, H. (2018). Eco-friendly polyvinyl alcohol/carboxymethyl cellulose hydrogels reinforced with graphene oxide and bentonite for enhanced adsorption of methylene blue. *Carbohydrate Polymers*, 185: 1-11.
40. Varaprasad, K., Jayaramudu, T., and Sadiku, E. R. (2017). Removal of dye by carboxymethyl cellulose, acrylamide and graphene oxide via a free radical polymerization process. *Carbohydrate Polymers*, 164: 186-194.
41. Melo, B. C., Paulino, F. A., Cardoso, V. A., Pereira, A. G., Fajardo, A. R., and Rodrigues, F. H. (2018). Cellulose nanowhiskers improve the methylene blue adsorption capacity of chitosan-g-poly (acrylic acid) hydrogel. *Carbohydrate Polymers*, 181: 358-367.
42. Chakrabarti, S., and Dutta, B. K. (2005). On the adsorption and diffusion of methylene blue in glass fibers. *Journal of Colloid and Interface Science,* 286(2): 807-811.
43. Senthil Kumar, P., Abhinaya, R.V., Gayathri Lashmi, K., Arthi, V., Pavithra, R., Sathyaselvabala, V., Dinesh Kirupha, S., and Sivanesan, S. (2011). Adsorption of methylene blue dye from aqueous solution by agricultural waste: Equilibrium, thermodynamics, kinetics, mechanism and process design. *Colloid Journal,* 73(5): 651.
44. Aroguz, A. Z., Gulen, J., and Evers, R. H. (2008). Adsorption of methylene blue from aqueous solution on pyrolyzed petrified sediment. *Bioresource Technology,* 99(6): 1503-1508.
45. Rehman, M. S. U., Kim, I., and Han, J.-I. (2012). Adsorption of methylene blue dye from aqueous solution by sugar extracted spent rice biomass. *Carbohydrate Polymers,* 90(3): 1314-1322.
46. Kavitha, D., and Namasivayam, C. (2007). Experimental and kinetic studies on methylene blue adsorption by coir pith carbon. *Bioresource Technology,* 98(1): 14-21.
47. Ofomaja, A. E. (2008). Kinetic study and sorption mechanism of methylene blue and methyl violet onto mansonia (*Mansonia altissima*) wood sawdust. *Chemical Engineering Journal,* 143(1): 85-95.
48. Mahini, R., Esmaeili, H., and Foroutan, R. (2018). Adsorption of methyl violet from aqueous solution using brown algae *Padina sanctae*-crucis. *Turkish Journal of Biochemistry,* 43(6): 623-631.
49. Sharafzad, A., Tamjidi, S., and Esmaeili, H. (2021). Calcined lotus leaf as a low-cost and highly efficient biosorbent for removal of methyl violet dye from aqueous media. *International Journal of Environmental Analytical Chemistry,* 101(15): 2761-2784.
50. Halysh, V., Sevastyanova, O., Riazanova, A. V., Pasalskiy, B., Budnyak, T., Lindström, M. E., and Kartel, M. (2018). Walnut shells as a potential low-cost lignocellulosic sorbent for dyes and metal ions. *Cellulose,* 25(8): 4729-4742.